Multiscale Templating of Siloxane Gels via Polymerization-Induced Phase Separation†

Kazuki Nakanishi,*,‡ Tomohiko Amatani,§ Seiji Yano,§ and Tetsuya Kodaira△

Department of Chemistry, Graduate School of Science, Kyoto University, Kitashirakawa, Sakyo-ku, Kyoto 606-8502, Japan, Department of Material Chemistry, Graduate School of Engineering, Kyoto University, Nishikyo-ku, Kyoto 615-8510, Japan, and National Institute of Science and Technology, 1-1-1, Higashi, Tsukuba-shi, Ibaraki 305-8565, Japan

Received August 31, 2007. Revised Manuscript Received November 8, 2007

By combining the micellar templating in nanometer-scale with the polymerization-induced phase separation in micrometer-scale, we can synthesize monolithic silica or silsesquioxane gel materials with hierarchical well-defined macropores and shape-controlled mesopores. Depending on the mechanism of enhancing micellar-templating of siloxane oligomers, macroframeworks containing long-range-ordered cylindrical mesopores with different degrees of order have been produced. Alkylene-bridged silicon alkoxides can also be prepared into similarly hierarchical porous structures with broadened variations in framework morphology. These examples demonstrate the versatility of using phase-separation in micellar-templated gelling systems to obtain well-defined macroporous structures.

Introduction

Architecture on the nanoscale utilizing micellar templating has been extensively explored in recent years.[1–4] The category of mesoporous materials now has a vast number of families in both structure and chemical composition. Materials in the forms of precipitates, nanoparticles in controlled shape, thin films with controlled orientation of pores, and macrosized monolith have been reported.[5–10] On the application side, the highly regulated pores are expected to be useful as supports for catalyst, on which introduced external molecules are decomposed or reacted with other molecules, and, importantly, the products must be transported away to accommodate the following reactants. The requirement for the efficient transport of molecules through the active surfaces of mesoporous materials is equally important in other applications such as separation media for gas/liquid chromatography. For an efficient contact of the internal surfaces with external substances, in situ generation of mesoporous materials in microfabricated channels or preformed macroporous arrays is a promising candidate.

Fabrication of monolithic macroporous materials with continuous pores typically in the range of micrometer−millimeters is recently becoming popular, especially as a scaffold for bone and tissue repair in medical applications.[11–15] Inspired mainly by biological systems, the importance and feasibility of integrating mesoporous structural units into macroporous frameworks to generate hierarchically porous organization have been extensively recognized.[16–18] Most macropore forming processes utilize the sacrificial templates of preformed decomposable substance such as polystyrene latex,[19–22] starch or other polymers, and stabilized emulsions.[23] In the cases of beads and emulsions, where the spaces occupied by assembled templates, ordered or disordered, are

† Part of the "Templated Materials Special Issue".

* Corresponding author. Phone: 8175-753-2925. Fax: 8175-753-2925. E-mail: kazuki@kuchem.kyoto-u.ac.jp.

‡ Graduate School of Science, Kyoto University.

§ Graduate School of Engineering, Kyoto University.

△ National Institute of Science and Technology.

(1) Kresge, C. T.; Leonowicz, M. E.; Roth, W. J.; Vartuli, J. C.; Beck, J. S. *Nature* **1992**, *359*, 710–712.
(2) Inagaki, S.; Fukushima, Y.; Kuroda, K. *J. Chem. Soc., Chem. Commun.* **1993**, *68*, 0–682.
(3) Beck, J. S.; Vartuli, C.; Roth, W. J.; Leonowicz, M. E.; Kresge, C. T.; Schmitt, K. D.; Chu, C. T-W.; Olson, D. H.; Sheppard, E. W.; McCullen, S. B.; Higgins, J. B.; Schlenker, J. L. *J. Am. Chem. Soc.* **1992**, *114*, 10834–10843.
(4) Soler-Illia, G. J. A. A.; Crepaldia, E. L.; Grosso, D.; Sanchez, C. *Curr. Opin. Colloid Interface Sci.* **2003**, *8*, 109–126.
(5) Antonietti, M.; Berton, B.; Goltner, C.; Hentze, H. P. *Adv. Mater.* **1998**, *10*, 154.
(6) Lebeau, B.; Fowler, C. E; S, M.; Farcet, C.; Charleux, B.; Sanchez, C. *J. Mater. Chem.* **2000**, *10*, 2105.
(7) Rhodes, K. H.; Davis, S. A.; Caruso, F.; Zhang, B. J.; Mann, S. *Chem. Mater.* **2000**, *12*, 2832.
(8) Yin, J. S.; Wang, Z. L. *Appl. Phys. Lett.* **1999**, *74*, 2629.
(9) Xu, L.-Y.; Shi, Z.-G.; Feng, Y.-Q. *Microporous Mesoporous Mater.* **2007**, *98*, 303.
(10) Brinker, C. J.; Lu, Y.; Sellinger, A.; Fan, H. *Adv. Mater.* **1999**, *11*, 579.
(11) Schmidt-Winkel, P.; Lukens, W. W.; Yang, P. D.; Margolese, D. I.; Lettow, J. S.; Ying, J. Y.; Stucky, G. D. *Chem. Mater.* **2000**, *12*, 686–696.
(12) Bagshaw, S. A. *Chem. Commun.* **1999**, *9*, 767.
(13) Zhang, B. J.; Davis, S. A.; Mann, S. *Chem. Mater.* **2002**, *14*, 1369.
(14) Studart, A. R.; Gonzenbach, U. T.; Tervoort, E.; Gauckler, L. J. *J. Am. Ceram. Soc.* **2006**, *89*, 1771–1789.
(15) Kitamura, M.; Ohtsuki, C.; Ogata, S.; Kamitakahara, M.; Tanihara, M. *Mater. Trans.* **2004**, *45*, 983–988.
(16) Mann, S.; Burkett, S. L.; Davis, S. A.; Fowler, C. E.; Mendelson, N. H.; Sims, S. D.; Walsh, D.; Whilton, N. T. *Chem. Mater.* **1997**, *9*, 2300–2310.
(17) Ozin, G. A. *Chem. Commun.* **2000**, *6*, 419–432.
(18) Soler-Illia, G. J. A. A.; Sanchez, C.; Lebeau, B.; Patarin, J. *Chem. Rev.* **2002**, *102*, 4093–4138.
(19) Lebeau, B.; Fowler, C. E.; Mann, S.; Farcet, C.; Charleuxc, B.; Sanchez, C. J. *Mater. Chem.* **2000**, *10*, 2105–2108.
(20) Li, Q. L.; Bai Yang, B.; Zhao, D. *Chem. Lett.* **2000**, *37* 8–379. PS Hard template.
(21) Sen, T.; Tiddy, G. J. T.; Casci, J. L.; Anderson, M. W. *Angew. Chem., Int. Ed.* **2003**, *42*, 4649–4653.
(22) Zhou, Y.; Antonietti, M. *Chem. Commun.* **2003**, 2564–2565.
(23) Imhof, A.; Pine, D. J. *Nature* **1997**, *389*, 948–951.

10.1021/cm702486b CCC: $40.75
Published on Web 12/28/2007

converted into macropores, whereas solid walls are formed at the interstices among the templates. As a result, although the total porosity can be considerably high, the connectivity among the individual macropores is not always high. From the viewpoint of flow resistance through the macroporous network, large pore spaces connected by narrower channels offer poor advantage because they give only poor permeability. In addition, colloidal crystal templates generally suffer from structural defects such as cracks and slip planes, which make it difficult to organize defect-free macroporous materials in longer length scales. There also exist several methods that offer interconnected macropores and macroframeworks;[14,24] however, the precise control of pore size distribution and structural homogeneity is rather difficult. To date, precisely controlled hierarchically porous organization by macrotemplate is mostly limited to coatings or layered organizations.[18,25]

Polymerization-induced phase separation combined with the sol–gel transition that has been established in many inorganic or hybrid systems is a useful alternative to the above macrotemplating technologies.[16,17] Although it cannot be readily extended to millimeter-sized pores, the applicable pore size range covers from 100 nm well more than 30 μm, which can be used in many separation/purification purposes of small molecules, polymers, and even larger biological entities such as proteins and cells. The method has initially been developed for amorphous inorganic phases such as silica and silica-based complex oxides. Sharply distributed, still amorphous, mesopores could be prepared within the macroframeworks by the postgelation aging process. However, it was not possible until recently to induce the phase separation by the surfactant additives themselves, which also template the mesopores. The macropore formation by phase-separation in micellar-templating systems and the macrotemplating of micellar-templated molecular assemblage is critically different from each other. The former requires no preformed space for the precursor materials to be molded, but the whole macroframeworks and macropores are developed by spontaneous and controllable process.

Considering that a lot of excellent reviews on hierarchically porous materials have been already published in the fields of colloidal, emulsion, and biological macrotemplating,[16–18] the present review will be devoted to the recent advances on the multiscale templating by the sol–gel process accompanied by phase separation. The macropore-forming process of polymerization-induced phase separation is combined with micellar-templated oxide and hybrid systems, taking pure silica and alkylene-bridged silsesquioxane as examples.

Experimental Section

Materials Synthesis. Most sample gels were synthesized via hydrolysis and polycondensation of metal alkoxides under acid-catalyzed and closed conditions. In the case of incorporating surfactants or water-soluble polymers, starting materials other than alkoxide were first mixed and homogenized. In the following examples, triblock copolymers known as Pluronic P123 and F127, having the molecular formulas of $(EO)_{20}(PO)_{70}(EO)_{20}$ and $(EO)_{106}(PO)_{70}(EO)_{106}$, respectively, were used as structure-directing agents as well as phase-separation inducers (EO, oxyethylene; and PO, oxypropylene units). The alkoxide was finally added to the premixed solution under vigorous stirring for hydrolysis. The temperature history was carefully controlled to be as common as possible in making comparison among the samples with systematic variations in starting compositions. The reaction solution thus prepared were transferred to closed vessels and kept at constant temperatures, typically 40–60 °C, for gelation. After gelation, the sample was subsequently aged in the same vessel to stabilize the structure. The postgelation solvent exchange was adopted when additional tailoring of mesopore structure was required. In the case of gel samples with micrometer-range continuous pores, the exchange of pore liquid with an external solution was performed efficiently and had a negligible effect on the preformed macroporous framework. The removal of volatile components was carried out by evaporation. Finally the gels were heat-treated at elevated temperatures, typically 550–650 °C for 2–5 h to completely decompose organic components. In the case of alkylene-bridged materials, heat-treatment was conducted at 300 °C for 5 h for the purpose of preserving organic parts in the hybrid network and decomposing only unnecessary components without damaging the materials structure.

Materials Characterization. Structural characterization was carried out mostly for gelled specimens in the absence of solvent-phase after drying and/or heat-treatment. A scanning electron microscope equipped with energy-dispersive X-ray analyzer (SEM-EDX: JSM-6060S + JED-2300, JEOL Ltd., Japan) and a field-emission scanning electron microscope (FE-SEM: JSM-6700F, JEOL Ltd., Japan) were used to examine morphologies of porous specimens using their fractured surfaces. Pore size distributions were measured using mercury porosimetry (PORESIZER-9320, Micromeritics Co.) for pores larger than 10 nm and nitrogen adsorption measurements (ASAP-2010, Micromeritics Co.) for pores smaller than 50 nm in diameter. The heat-treated samples were degassed under 5 μm Hg reduced pressure at 200 °C for 1 h prior to the measurements to remove physically adsorbed water. The specific surface area was calculated by the Brunauer–Emmett–Teller (BET) method and the distribution of mesopores was calculated by Barrett–Joyner–Halenda (BJH) method using the adsorption branch of the isotherm. Optional transmission electron microscope (TEM) observation and high-resolution X-ray diffraction (XRD) measurements were also performed using Ni-filtered Cu Kα radiation.

Background and Principles

With the systems containing tetraalkoxysilane and appropriate additives as a starting point, the polymerization-induced phase separation, especially the spinodal decomposition, has been extensively utilized to generate well-defined heterogeneous structures.[26,27] In most cases, the hydrolysis is conducted under acidic conditions where a relatively narrow distribution of growing oligomers can be obtained.[28] Although the polymerization reaction is conducted at a constant temperature, the phase separation is induced by the polymerization reaction itself.[29] The simplified free energy change of mixing multiple constituents in a solution, ΔG, can be written as

$$\Delta G = \Delta H - T\Delta S \quad (1)$$

(24) Maekawa, H.; Esquena, J.; Bishop, S.; Solans, C.; Chmelka, B. F. *Adv. Mater.* **2003**, *15*, 591–596.
(25) Sanchez, C.; Arribart, H.; Giraud Guille, M. M. *Nat. Mater.* **2005**, *4*, 277–288.
(26) Nakanishi, K. J. *Porous Mater.* **1997**, *4*, 67–112.
(27) Nakanishi, K; Tanaka, N. *Acc. Chem. Res.* **2007**, *40*, 863–873.
(28) Brinker, C. J.; Scherer, G. W. *Sol−Gel Science; The Physics and Chemistry of Sol−Gel Processing*; Academic Press: New York, 1990; pp 108–216.
(29) Flory, P. J. *Principles of Polymer Chemistry*; Cornell University Press: Ithaca, NY, 1971.

When the sign of ΔG becomes positive, the thermodynamic driving force for phase separation is generated. The polymerization among any constituents usually reduces the ΔS term by decreasing the freedom in chemical configurations, whereas the physical cooling of the system is expressed by the reduction in T. In either case, the absolute value of the $T\Delta S$ term decreases and the phase separation is equivalently induced.[30] The polymerization can be regarded as a "chemical cooling" process with this respect. In practice, poor solvents of the oligomers, several kinds of water-soluble polymers, and surfactants can be used as an inducer of the phase separation driven by the polymerization reaction.

Sol–gel systems depicted here undergo a phase separation to generate micrometer-range heterogeneity composed of gel and fluid phases. After the solidification (gelation) of the whole system, the fluid phase can be removed relatively easily to leave pore spaces in the length scale of micrometers. In many cases of thermally induced phase separation in metallic alloys, polymer blends, and multicomponent glasses, the kinetics of phase separation can be externally controlled through temperature. One can quench the shape and size of the developing phase domains simply by cooling the system. On the other hand, the structure formation process has a more or less spontaneous nature in the present sol–gel systems. Both the onset of phase separation and sol–gel transition are governed by the kinetics of chemical bond formation. With a predetermined composition, the homogeneously dissolved starting constituents are just left to react at a constant temperature in a closed condition (to avoid evaporation of volatile components). It is noteworthy that not a few gel-forming systems exhibit common features of concurrent phase separation and sol–gel transition, regardless of the difference in the origins of their gel-forming reactions.

When the phase separation is induced in the unstable region of a phase diagram (a temperature-composition region within the spinodal curve), a specific process called spinodal decomposition occurs. With comparable volume fractions of conjugate phase domains without crystallographic or mechanical anisotropy, a cocontinuous structure forms. The cocontinuous structure is characterized by mutually continuous conjugate phase domains and hyperbolic interfaces.

The final morphology of the spinodally decomposed phase domains is strongly governed by the dynamics driven by the interfacial energy.[31] The well-defined cocontinuous structure of the spinodal decomposition is a transient one, which coarsens self-similarly for a limited duration of time and then breaks up into fragments. To reduce the total interfacial energy, the system reorganizes the domain structure toward that with less interfacial area and less local interfacial energy. Within the regime of self-similar coarsening, the geometrical features of the developing domains remain unchanged except the characteristic size. It is then followed by the fragmentation of the either of the continuous domains, which results in the dispersion of one phase within the other continuous phase.

Sol–gel transition is a dynamical freezing process that occurs via cross-linking reactions. If any transient (dynamic) heterogeneity is present in a gelling solution, it will be arrested in a gel network if the time scale of a sol–gel transition is short enough to take the snapshot of the transient heterogeneity. The "frozen" structure depends, therefore, on the onset of phase separation relative to the "freezing" point by sol–gel transition. The earlier the phase separation is initiated relative to the sol–gel transition, the coarser the resultant structure becomes, and vice versa. For example, a higher reaction temperature normally increases the mutual solubility of the constituents and hence suppresses the phase separation tendency, and in parallel it accelerates the hydrolysis/polycondensation reactions. As a result, the onset of phase separation is retarded and the solution is solidified earlier by the sol–gel transition. Because of these duplicate effects, gels with drastically finer phase-separated domains are obtained at higher temperatures. With an appropriate choice of the reaction parameters such as starting composition and temperature, the pore size (domain size) and pore volume of the gels can be designed over a broad range.

In the following sections, as we deal mainly with the internal structure of gel-domains, the term "macroframeworks" will be used instead of the frequently used term "skeletons". The term "skeleton" is indeed inappropriate in the cases of extraordinary modified continuous gel phase shown in the last section, even though their internal structure sometimes looks very similar to the networked porous textures of real bones.

Incorporation of Templated Mesopores into Macroframeworks

As has been experimentally evidenced, the macroframeworks formed by the phase separation/sol–gel transition process can be consisted of infinitely cross-linked polymer (organic, inorganic, or hybrid), colloidal particles or micellar-templated gel networks.[27] The only prerequisite for the formation of well-defined macroframeworks and continuous macropores is simply a competitive occurrence of phase separation and sol–gel transition. The macroframework is formed without any assist of physical template, but via the spontaneous self-organization process of spinodal decomposition. Molecular-scale assemblies such as randomly polycondensed oligomers, colloidal aggregates, or micellar-templated oligomers are preserved when they are frozen into the network of self-organizing macroframeworks.

Because the induction of phase separation is possible in many alkoxy-derived systems by an incorporation of surfactant, micellar-templating with a lower degree of structural order such as wormholelike pores is readily possible.[32,33] Pores with narrow size distribution are the results of random aggregation of individual micelles adsorbed by the silica oligomers. There exists only a strong nearest-neighbor correlation among the pores and no periodicity in the longer length scale is recognized. Similar type of macroporous silica with randomly oriented uniform mesopores is reported in a system incorporated with poly(ethylene glycol) and cetyltrimethylammonium bromide.[34] To obtain mesopores with higher degree of structural orders, one needs to enhance the mutual alignment of templated oligomers within the macroframeworks. In the case of rodlike micelles, the enhancement of mutual alignment is expectedly closely related to the formation of stabilized longer and straight micelles. That is, with an increase of the length of straight individual rodlike micelles, there arises stronger lateral interaction to align them in higher degree of order.

Experimental evidence observed in both pure silica and ethylene-bridged polysilsesquioxane systems commonly prove this mecha-

(30) deGennes, P. G. *Scaling Concepts in Polymer Physics*; Cornell University Press: Ithaca, NY, 1979; p 73.
(31) Hashimoto, T.; Itakura, M.; Hasegawa, H. J. *Chem. Phys.* **1986**, *85*, 6118–6128.
(32) Sato, Y.; Nakanishi, K.; Hirao, K.; Jinnai, H.; Shibayama, M.; Melnichenko, Y. B.; Wignall, G. D. *Colloids Surf., A* **2001**, *187/188*, 117–122.
(33) Nakanishi, K.; Sato, Y.; Ruyat, Y.; Hirao, K. J. *Sol−Gel Sci Technol.* **2003**, *26*, 567–570.
(34) Smått, J.-H.; Schunk, S.; Lindén, M. *Chem. Mater.* **2003**, *15*, 2354–2361.

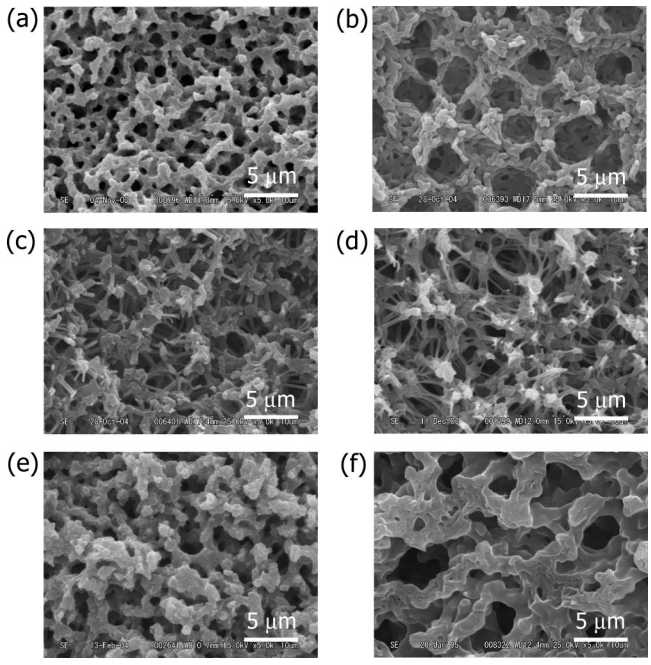

Figure 1. SEM photographs of heat-treated gels prepared in the system of TMOS-P123–1 M HNO_3 (aq) with varied amounts of TMB. Starting compositions are shown in Table 1. (a) MP4, (b) MP4-T045, (c) MP4-T085, (d) MP4-T090, (e) MP4-T125, (f) MP4-T310.

Table 1. Starting Composition of the Gel Samples in TMOS−P123–1.0 M HNO_3 (aq)−TMB System (g) (reaction temperature = 60 °C)

sample	TMOS	P123	TMB	1.0 M HNO_3 (aq)
MP4	5.15	4.0		12.0
MP4-T045	5.15	4.0	0.45	12.0
MP4-T065	5.15	4.0	0.65	12.0
MP4-T085	5.15	4.0	0.85	12.0
MP4-T090	5.15	4.0	0.90	12.0
MP4-T125	5.15	4.0	1.25	12.0
MP4-T310	5.15	4.0	3.10	12.0

nism. Figure 1 shows morphological change with additions of trimethylbenzene (TMB) to the starting composition which gives macroporous morphology with disordered mesopores.[35] The starting compositions are listed in Table 1. With increasing additions of TMB, initially isotropic cocontinuous macroframeworks once coarsen and then exhibit fibrous appearance. The nitrogen adsorption isotherms (Figure 2) and XRD profiles (not shown) evidenced that the development of straight cylindrical pores with the 2D hexagonal symmetry concurs with the emergence of fibrous macroframeworks. Here, TMB works not only as a pore expander but also to enhance the interactions among the hydrophobic moieties of the structure-directing agent, Pluronic P123. Further additions of TMB, however, oversaturate the micelles in the form of cylinders, and the P123 are reorganized into spherical droplets. The resulting structure becomes the mesostructured cellular foams (MCF)[11] without any crystallographic orientation (Figure 2).

During the above mesoscopic transitions from wormhole, via cylindrical, to spherical geometries, the silica macroframeworks transforms from isotropic, via fibrous, and again isotropic, without significant change in their characteristic size (defined by the sum of overall thickness of the framework and the pore diameter). This implies that the mesoscopic anisotropy of P123 micelles induced by the incorporation of TMB is superimposed over the existing morphology of the macroframeworks. Alternatively, it is possible that originally randomly oriented cylindrical molecular assemblies are forced to align along the length of columnar macroframeworks in the coarsening stage of the phase separation. In any case, the concurrence among (1) polymerization-induced phase separation, (2) cooperative assembly of the surfactant micelles and silica oligomers, and (3) sol–gel transition is realized in the above results.

Spinodal decomposition mechanism describes only the driving force of domain formation induced by the phase separation under the thermodynamically unstable conditions. As described in the preceding section, with the development of compositional contrast between the neighboring phase domains, surface energy plays increasingly important roles in determining the final morphology of the whole material.[31] On the other hand, anisotropy in atomic or molecular scale is also known to affect the overall morphology of the phase domains. Metallic alloys that are consisted of cocontinuous domains usually exhibit anisotropies related to the crystallographic orientations of the constituents of respective phase domains. The effect of anisotropy as well as the energetic contribution of elastic strains thereof has been discussed already in the early theoretical study of the spinodal decomposition.[36,37] With this regard, the addition of TMB to the phase-separating P123-TMOS induces an internal structural order by giving "crystallinity" to the cooperative assembly of surfactant micelles and silica oligomers.

Controlling Macroassemblage of Micellar-Templated Structural units

In the similar experimental system to the above examples, another type of multiscale templating is also possible. Under the specific conditions where the micellar-templated oligomers exhibit strong structural anisotropy arising from their high degree of order, the local morphology of the macroframeworks are governed by the crystallographic orientation of highly ordered aggregates. By increasing the relative amount of water containing a fixed concentration of acid catalyst, one can observe a morphological transformation that follows a different path from that of TMB additions described above (Figure 3). A relatively small increase in the water concentration gives coarser phase-separated domains, which is, in many other systems without structure-directing agents, usually followed by the macroscopically separated two-phases at higher water concentrations. In the P123−TMOS system, however, we observed the generation of continuous macroframeworks consisting of nearly an order finer structural units. This result is essentially different from those observed with TMB additions where the macroframeworks transformed into anisotropic in shape but dimesion of macroframeworks as a whole was essentially unaffected. Careful examination into these submicrometer structural units reveals that these "particles" have broad distribution in size and shape at relatively lower water concentration, but that both the size and shape become more uniform with an increase in the water concentration. The emergence of uniform-sized particles in the shape of "rice grain" nearly parallels the formation of straight cylindrical pores in 2D hexagonal symmetry evidenced by nitrogen adsorption isotherms and XRD profiles. At higher water concentrations, the median size of cylindrical mesopore gradually increases without deteriorating the cylindrical pore shape and their long-range orders. Above the molar ratio water/Si > 100, the overall morphology transformed into that composed of thin continuous mesoporous strands (Figure 3d). In this extreme morphology, the porosity by macropores well exceeds 90% by volume (Figure 4), whereas the cylindrical mesopores are present in the thin rod-shaped silica

(35) Amatani, T.; Nakanishi, K.; Hirao, K.; Kodaira, T. *Chem. Mater.* **2005**, *17*, 2114–2119.
(36) Cahn, J. W. *Acta Metall.* **1961**, *9*, 795–801.
(37) Cahn, J.W. J. *Chem. Phys.* **1965**, *42*, 93–99.

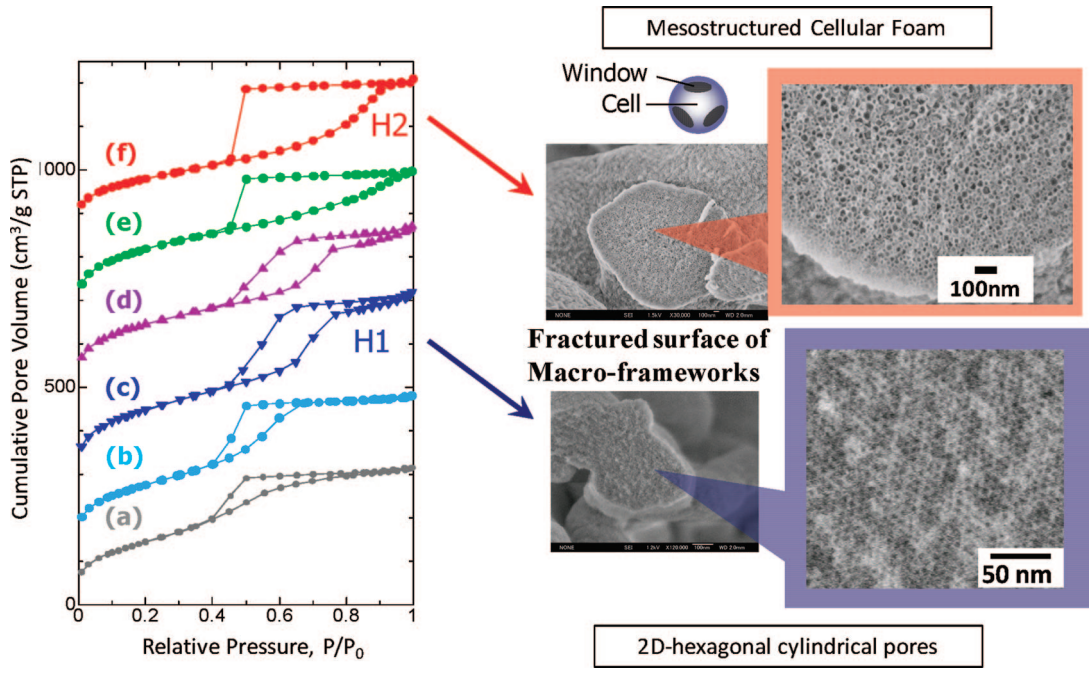

Figure 2. Nitrogen adsorption isotherms (left) of heat-treated gels prepared in TMOS-P123–1 M HNO_3 (aq)−TMB system and corresponding morphologies of macroframeworks (center) and magnified image (right) highlighting the difference in mesoporous structures. Sample notations are the same as in Figure 1.

Table 2. Starting Composition of the Gel Samples in TMOS−P123–1.0 M HNO_3 (aq) System (g) (reaction temperature = 60 °C)

sample	TMOS	P123	1.0 M HNO_3aq
MP4-W12	5.15	4.0	12.0
MP4-W14	5.15	4.0	14.0
MP4-W20	5.15	4.0	20.0
MP4-W28	5.15	4.0	28.0
MP4-W36	5.15	4.0	36.0
MP4-W44	5.15	4.0	44.0
MP4-W84	5.15	4.0	84.0

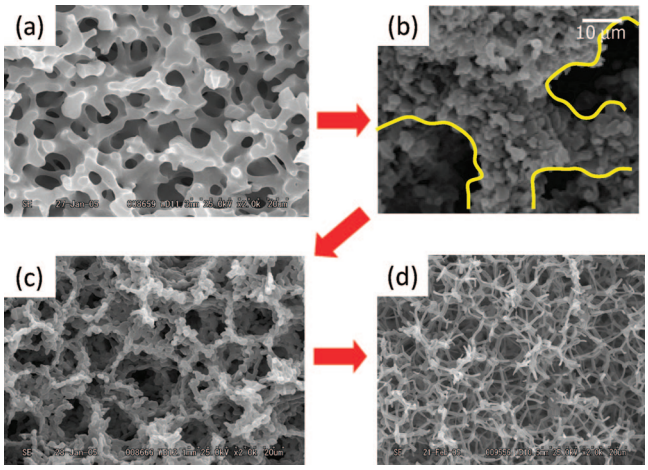

Figure 3. Morphological transformation of macroframeworks in the system of TMOS−P123–1 M HNO_3 (aq). Starting compositions are shown in Table 2. (a) MP4-W14, (b) MP4-W20, (c) MP4-W44, (d) MP4-W84.

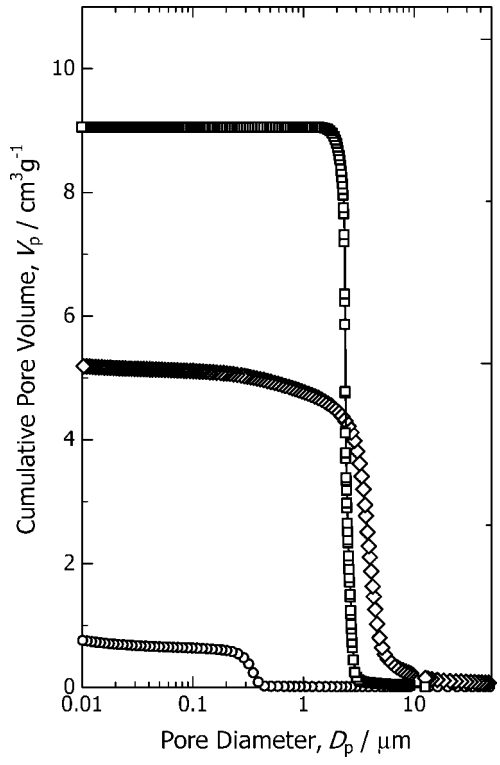

Figure 4. Cumulative pore size distribution of heat-treated gels in the system of TMOS−P123–1 M HNO_3 (aq) measured by mercury porosimetry: circle, MP4-W12; diamond, MP4-W44; square, MP4-W84.

skeletons (Figure 5). The corresponding XRD profile (Figure 6) exhibits highly ordered 2D hexagonal arrangement indicating that each mesoporous macroframework is a "single-crystal" composed of cylindrical pores and pore walls as confirmed by TEM observation (Figure 7).

Precipitation of crystallographically oriented micellar-templated silica has been reported already in the early paper on mesoporous silica.[3] Since the short-chain alcohols generated by the hydrolysis of alkoxysilanes most probably disturb the stable cooperative assembly of surfactant micelles and silica oligomers, mesoporous materials with high long-range order have been synthesized with abundant water or by preferential removal of alcohols in the preparation process. Control over the aggregation of cooperatively assembled micellar-templated oligomers becomes possible in the copresence of relatively high concentration of surfactant that makes the viscosity of the gelling solution considerably high. Although

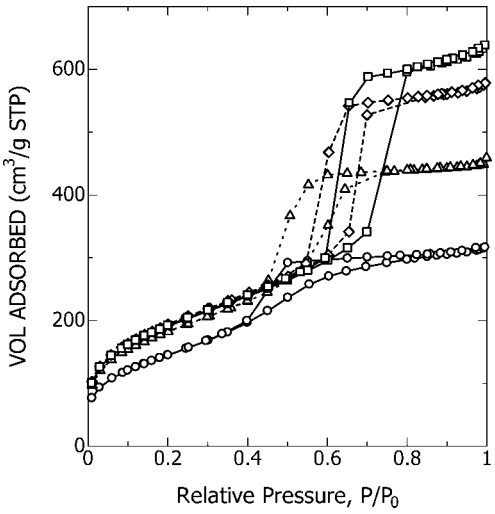

Figure 5. Nitrogen adsorption–desorption isotherms of heat-treated gels in the system of TMOS−P123–1 M HNO_3 (aq): circle, MP4-W12; triangle, MP4-W28; diamond, MP4-W44; square, MP4-W84.

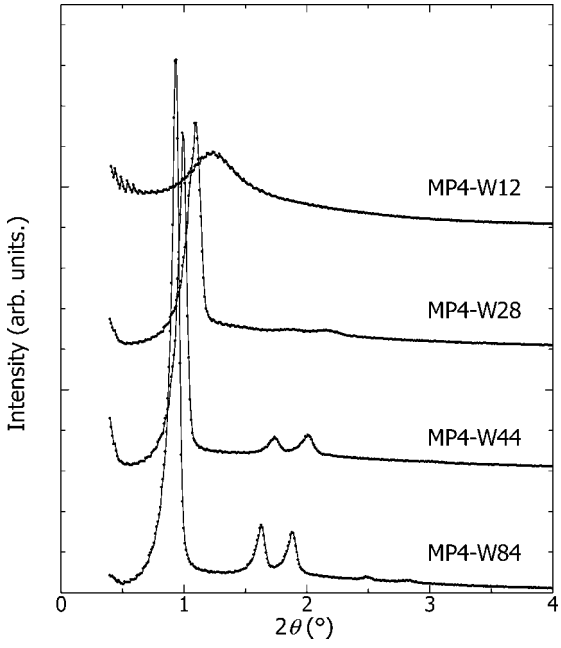

Figure 6. X-ray diffraction profiles of heat-treated gels in the system of TMOS−P123–1 M HNO_3 (aq). From the lower diffraction angles, peaks in each profile can be indexed to 10, 11, 20, 21, and 30 diffractions of 2D hexagonal symmetry. The diffraction peaks of MP4-W84 are most clearly resolved, showing the highest long-range order of mesopores. Intensities are arbitrarily shifted for clarity.

the resultant macroframeworks seem substantially similar to each other in shape, TMOS−P123 systems synthesized with additions of TMB and those with abundant amount of water follow different paths to generate macroframeworks with different degrees of long-range order. The use of silanes modified by polar compounds such as glycerols or ethylene glycols is reported to give similar macroporous materials with long-range-ordered mesopores to those obtained in the present TMOS-P123 system with abundant water.[38,39]

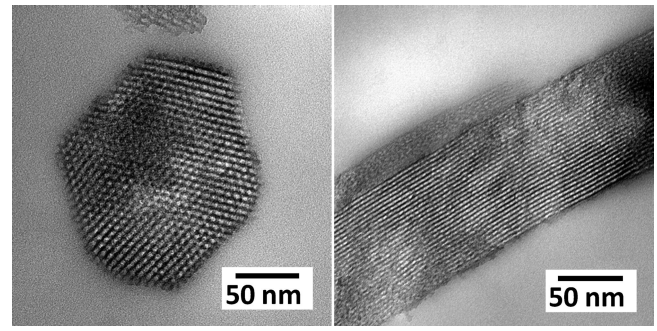

Figure 7. Transmission electron micrographs of macroframework of the heat-treated gel prepared in the system of TMOS−P123–1 M HNO_3 (aq). The starting composition is MP4-W84.

Ethylene-Bridged Silsesquioxane

Bridged alkoxysilanes such as bis(trialkoxysilyl)alkanes are known to give mesoporous materials via similar cooperative assembly with surfactant micelles to those observed in pure silica systems.[40] In a typical case of bis(trimethoxysilyl)ethane, BTME, the incorporation of P123 together with TMB also results in the formation of hexagonally aligned mesopores within the macroframeworks formed via the polymerization-induced phase separation.[41] The transformation in mesoscopic scale from cylindrical to MCF-type pores is also observed with further additions of TMB. Moreover, with a higher concentration of water, typically a water/Si molar ratio exceeding 100, gels with similar macroframeworks containing "single-crystal-like" well-aligned mesopores as shown above (Figure 3) are also obtained. This similarity between TMOS and BTME in forming micellar-templated macro/mesoporous monolithic gels is almost surprising. The silicon−carbon bonds consisting ideally of 25% of the whole cross-links give BTME-derived gels much higher alkaline resistance compared with pure silica gels. Partial or total replacement of macro/mesoporous materials with BTME-derived network is promising in developing applications such as separation media for HPLC in controlling alkaline resistance while maintaining advantageous surface properties of pure silica.[42]

In addition to the typical cases with Pluronic P123, the structural regulation using Pluronic F127 has also been found to be possible in BTME-derived systems. Regulation of micelle length and resultant morphology of the framework is performed by the concentrations of additives (cosurfactants). Using somewhat complex starting constituents composed of BTME-F127, TMB, and benzyl alcohol under acid-catalyzed conditions, the unusual shape of macroframeworks can be developed[43] (Figure 8). Although the detailed mechanisms still remain unclear, the benzyl alcohol seems to work as a cosurfactant as well as a micelle-length regulator in a limited composition range. While maintaining the highly 2D hexagonally ordered cylindrical pores, the structural units of macroframeworks transform from thin disk, via short column, to a long straight column. In this case also, all the materials are obtained fully interconnected in micrometer range (monolithic form) and can be shaped into a broad range of geometries and dimensions.

(38) Brandhuber, D.; Hüsing, N.; Raab, C. K.; Torma, V.; Peterlik, H. *J. Mater. Chem.* **2005**, *15*, 1801–1806.
(39) Hartmann, S.; Brandhuber, D.; Hüsing, N. *Acc. Chem. Res.* **2007**, *40*, 885–894.
(40) Inagaki, S.; Guan, S.; Fukushima, Y.; Ohsuna, T.; Terasaki, O. *J. Am. Chem. Soc.* **1999**, *121*, 9611–9614.
(41) Nakanishi, K.; Kobayashi, Y.; Amatani, T.; Hirao, K.; Kodaira, T. *Chem. Mater.* **2004**, *16*, 3652–3658.
(42) Wyndham, K. D.; O'Gara, J. E.; Walter, T. H.; Glose, K. H.; Lawrence, N. L.; Alden, B. A.; Izzo, G. S.; Hudalla, C. J.; Iraneta, P. C. *Anal. Chem.* **2003**, *75*, 6781–6788.
(43) Yano, S.; Nakanishi, K.; Hirao, K.; Kodaira, T. Unpublished data.

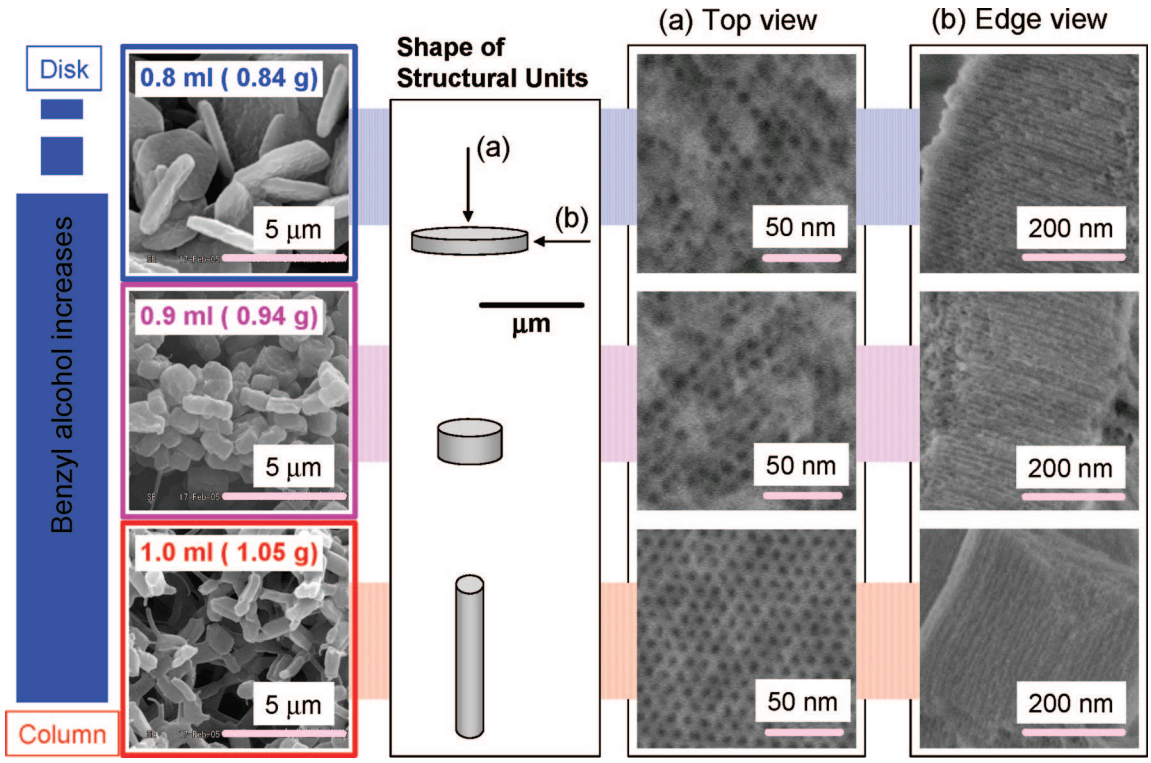

Figure 8. Morphological transformation of macroframeworks in BTME-F127-TMB system incorporated with varied amounts of benzyl alcohol. The starting compositions are listed in Table 3. Left row shows overall morphology of the macroframework; to the right, schematic drawings of the structural units, top view of the individual structural units by FE-SEM showing 2D-hexagonal arrangement of cylindrical pores, edge view of the structural units showing that cylindrical pores are aligned in the direction of thickness (disk) or length (column) of the macroframeworks.

Potential Application As a Novel Monolithic HPLC Column

Pure silica gels with cocontinuous macropores and regulated-size mesopores without long-range order have been applied to separation media for HPLC.[44,45] The independent control over the macroporosity and thickness of macroframeworks, compared with tightly packed uniform-sized spherical gel particles that always give 40% porosity at highest, offered several advantages, especially for fast separation purposes. On the optimum geometry of the gel skeletons, however, it has not been fully established which combination of thickness of macroframeworks, macroporosity, and mesopore size (possibly the mesopore symmetry) is the best for each targeted separations. Computational fluid dynamics simulation predicts that exceedingly high porosity in a column does not always contribute to better performance even if the geometries of macroframeworks and macropores are highly regulated.[46,47] Experimental works to precisely evaluate macro/mesoporous silica (or silsesquioxane) monoliths as HPLC separation media is still required to elucidate the comprehensive answer to the question; "What is the best available structure via sol−gel synthesis for the ultimate HPLC separation?" Novel quantitative methods of structural characterization of macroframeworks in connection with computational fluid dynamics simulation will help to optimize the macropore structure.[48,49] On the other hand, experimental evidence has shown, using mesoporous particles and monoliths, that the rate of material transfer within the stationary phase is accelerated in chromatographic separations.[50] The highly tenuous structures obtained in silica and BTME systems with highly ordered mesopores offers the additional possibility of developing a new class of separation medium with further improved performance.

Table 3. Starting Composition of the Gel Samples in the BTME−F127–0.1 M HNO_3 (aq)−TMB System (g) (reaction temperature = 60 °C)

sample	BTME	F127	0.1 M HNO_3aq	TMB	benzyl alcohol
thin disk	2.15	1.40	10.79	0.35	0.84
short column	2.15	1.40	10.79	0.35	0.94
long column	2.15	1.40	10.79	0.35	1.05

Conclusions

Among various possibilities to integrate micellar-templated mesoporous materials into macroporous assemblies, the polymerization-induced phase separation and sol–gel transition offers a wide spectrum of materials specifications. With highly accessible mesopore arrays with regulated size and shape, further improved monolithic HPLC separation media will be the most promising application. An extraordinarily high macroporosity does not always promise higher efficiency in HPLC separations; however, fast and efficient contact between the internal surfaces and external liquidus substances are realized. Solid-phase extractions routinely used in biochemistry will be much more accelerated by these

(44) Minakuchi, H.; Nakanishi, K.; Soga, N.; Ishizuka, N.; Tanaka, N. *Anal. Chem.* **1996**, *68*, 3498–3501.
(45) Tanaka, N.; Kobayashi, H.; Nakanishi, K.; Minakuchi, H.; Ishizuka, N. *Anal. Chem.* **2001**, *73*, 420A–429A.
(46) Gzil, P.; Vervoort, N. V.; Baron, G.; Desmet, G. *Anal. Chem.* **2004**, *76*, 6707–6718.
(47) Billen, J.; Gzil, P.; Desmet, G. *Anal. Chem.* **2006**, *78*, 6191–6201.
(48) Kanamori, K.; Nakanishi, K.; Hirao, K.; Jinnai, H. *Langmuir* **2003**, *19*, 5581–5585.
(49) Saito, H.; Nakanishi, K.; Hirao, K.; Jinnai, H. *J. Chromatogr., A* **2006**, *1119*, 95–104.
(50) Galarneau, A.; Iapichella, J.; Brunel, D.; Fajula, F.; Bayram-Hahn, Z.; Unger, K.; Puy, G.; Demesmay, C.; Jean-Louis Rocca, J. L. *J. Sep. Sci.* **2006**, *29*, 844–855.

highly permeable devices with active internal surfaces. As partly realized in commercial products, the materials shape is now selectable from large monoliths to smaller volume devices confined in 2D (coating), 1D (capillary), or 0D (individual dot) geometry. Further extension to oxide and metalloxane systems other than silica and siloxane is expected in the near future.

Acknowledgment. We thank Prof. Hiroshi Jinnai, Kyoto Institute of Technology, and his colleagues for TEM observation. This work was partly supported by the Grant for Practical Application of the University R&D Results under the Matching Fund Method from the New Energy and Industrial Technology Development Organization (NEDO), Japan.

CM702486B